



Farm soil moisture mapping using reflected GNSS SNR data onboard low level flying aircraft

L. Ameglio¹, J. Darrozes² and J. Dreyer³

1. GyroLAG, South Africa, laurent@gyrolag.com

2. University Paul Sabatier, CNRS, IRD, GET-OMP, GRGS, France

3. North West University, South Africa

**A paper from the Proceedings of the
14th International Conference on Precision Agriculture
June 24 – June 27, 2018
Montreal, Quebec, Canada**

Abstract. *Soil moisture/water content monitoring (spatial and temporal) is a critical component of farm management decision primarily for crop/plant growth and yield improvement, but also for optimization of practice such as tillage and field treatments. Satellite humidity probes do not deliver the relevant resolution for farming purposes. Ground moisture probes only provide punctual measurements and do not reflect the true spatial variability of soil moisture.*

Previous studies have demonstrated that variations of the nature of the ground/soil (i.e. moisture/water content amongst others parameters) modify the properties of reflected waves resulting in variations of amplitude and phase of the signal-to-noise ratio (SNR) recorded by a Global Navigation Satellite System (GNSS) receiver. Ground based studies analyzing the time variations of SNR measurements linked to dielectric constant of the surrounding soil established a method to recover local fluctuations of soil moisture content.

This method was adapted to airborne application and trialed on low level flying GyroLAG's light and affordable aircraft also used for other airborne remote sensing agri-surveying work (e.g. magnetic and gamma spectrometry soil zoning). Data processing chain was adjusted to the specifics of the airborne dynamic context. Spatial resolution of 45 m was achieved for the specific test conditions (120-140 km/hr flying speed and 50-100 m agl survey height). Comparison with isolated in situ measurements of soil moisture proved to be poor at less than 75% correlation. A second test is now planned to be performed over a single farm/pivot with validation over a regular grid of in situ measurements of soil moisture.

Keywords. *airborne, soil moisture mapping, GNSS-R, small aircraft, agriculture, environment.*

The authors are solely responsible for the content of this paper, which is not a refereed publication.. Citation of this work should state that it is from the Proceedings of the 14th International Conference on Precision Agriculture. EXAMPLE: Lastname, A. B. & Coauthor, C. D. (2018). Title of paper. In Proceedings of the 14th International Conference on Precision Agriculture (unpaginated, online). Monticello, IL: International Society of Precision Agriculture.

Introduction

The various stages of growth of crop/plant are a function of the soil moisture conditions (amongst other factors) with significant effects on the total growth and yield volume of a crop. Knowing how much water to apply to a field and when to apply it is then a fundamental management decision on which effective water management practices must be based. Furthermore, other practice such as tillage and field treatments can be optimized with real time knowledge of soil water content. Soil moisture monitoring (spatial and temporal) is consequently a critical component of agricultural production hence worldwide food supply sustainability.

International initiatives in satellite remote sensing such as the Soil Moisture and Ocean Salinity (SMOS) (Kerr *et al.* 2010), the International Soil Moisture Network (Dorigo *et al.* 2013) or the Committee on Earth Observation Satellites (CEOS) Land Product Validation group (Morissette *et al.* 2006) have provided such observations. However, they remain very sparse, are not timeous and do not provide the appropriate resolution to monitor land surface variables at a local scale. This is usually achieved by ground moisture probes. Those however only provide a punctual measurement which average (*e.g.* over 20 Ha surface) does not reflect the true spatial variability of soil moisture.

Recent studies demonstrated that Global Navigation Satellite System (GNSS) multipath signals can also be used to retrieve various geophysical parameters of the surface surrounding a GNSS receiving antenna (Motte *et al.* 2016a). Over land, variables such as soil moisture, snow depth and vegetation status can be observed when measured from static ground station (*e.g.* Roussel *et al.* 2016, Motte *et al.* 2016b, Chew *et al.* 2014). Soil moisture measurements are very important for climate studies, weather predictions, analyzes of floodplains or aquifers refill. Around 70 percent of worldwide freshwater is used by agriculture. To be able to feed an estimated additional 2 billion people by 2030, water demand is expected to increase tremendously in the next decades. Farmers are challenged to produce “more crop per drop”. In order to optimize water resource management (tillage treatments, irrigation), it is crucial to improve soil moisture situation awareness. In partnership with the GET laboratory team (France), an experiment of airborne detection of the soil moisture variations through GNSS reflectometry (GNSS-R) has being conducted on agricultural lands in the North-West region of South Africa. The airborne platforms, test protocol and initial results are presented in this paper.

GNSS-R principle

The GNSS-R is generally considered as an opportunistic remote sensing technique based on the analysis of the electromagnetic waves continuously emitted by GNSS constellation (GPS, GLONASS, Galileo, *etc*) that are received by an antenna after reflection on the Earth's surface, the so-called multipath (or MTP) signals (Darrozes *et al.* 2017, Roussel 2015) (see Fig. 1a). As multipath still represent a major problem for reaching precise GNSS positioning, the mitigation of their influence has been widely investigated. Different filtering measures affect the total received signal by reducing the reflected signals amplitude with respect to the direct signal amplitude. It is however well known that energy from reflected signal is not totally rejected. Variations of the nature of the surface is likely to modify the properties of the reflected waves, and consequently lead to variations of amplitude, phase and frequency of the Signal-to-Noise Ratio (SNR), *e.g.* recorded by a GNSS receiver. Let A_m and A_d be respectively the amplitudes of the MTP and direct signal, and ψ the phase difference between the two signals. Following Larson *et al.* (2007), and assuming that $A_m \ll A_d$, SNR at any instant can be described by:

$$SNR^2 = A_d^2 + 2 \cdot A_d \cdot A_m \cdot \cos(\varphi) \quad (1)$$

where SNR is the total SNR measured by the receiver, A_d is the amplitude of direct signal, A_m is the amplitude of the reflected signal and φ is the phase difference between direct and reflected

ones.

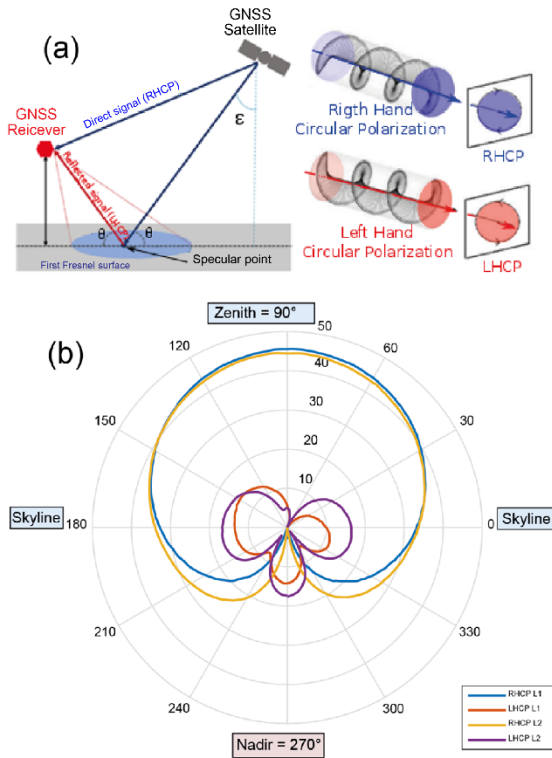


Fig. 1 Interactions between GNSS electromagnetic waves and reflecting surface: **(a)** GNSS measurements recorded by the receiver showing the direct path with Right-Hand Circular Polarization (RHCP) of the GNSS waves and the reflected path with Left-Hand Circular Polarization (LHCP); **(b)** Antenna gain pattern for the Right-Hand Circular Polarization (RHCP) and Left-Hand Circular Polarization (LHCP) for Leica AR10; modified from Darrozes *et al.* 2017

Equation 1 shows that overall magnitude of the SNR will be large and mainly driven by the low frequency direct signal whose variation will only be function of the satellite elevation angle (Darrozes *et al.* 2016). The reflected signal will affect the SNR by producing an intermediary frequency but small amplitude perturbation, which will particularly be visible for low satellite elevation angle (Fig. 2, green ellipse).

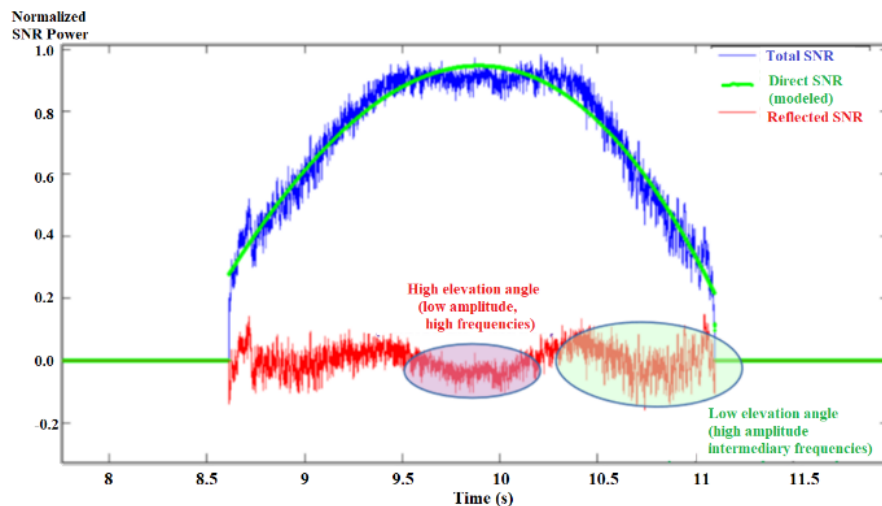


Fig. 2 Various SNR obtained from GPS satellite PRN12: measured total SNR (blue line), Direct SNR modelled using 2nd order polynomial function (green line), resulting Multipath SNR (Darrozes *et al.* 2016)

The SNR contribution (Equation 2) of the reflected signal (Fig. 2, red line) is isolated by removing modelled direct signal (Fig. 2, green line) and the remaining SNR_m can be defined as:

$$SNR_m = A \cdot \cos\left(\frac{4\pi \cdot h}{\lambda} \cdot \sin(\theta) + \phi\right) \quad (2)$$

where h is evaluated with a Lomb Scargle Periodogram, and then A and Φ are estimated with a Least Square Method (Darrozes *et al.* 2016). The three estimated parameters A , Φ and h , in most cases, show a direct correlation with soil moisture (Darrozes *et al.* 2016).

Airborne platform

Carriers

Two aircraft types were used for the airborne test: (1) a gyrocopter (see Fig. 3, see also Ameglio *et al.* 2015) and; (2) a sport fixed-wing aircraft, a Maule M5-235 (see Fig. 4).



Fig. 3 GyroLAG highly modified South African gyroplane Trojan equipped also with geophysical instruments.



Fig.4 GyroLAG fixed-wing Maule M5-235 aircraft

The main technical characteristics of the gyrocopter and fixed-wing aircraft used are presented in Table 1 and 2 respectively.

Table 1. Salient technical specifications of GyroLAG Trojan gyrocopter aviation platform.

Number of seats		2
Endurance (hrs)		> 4
Fuel consumption (litres/hr)		24 (unleaded 95)
Aircraft range (km)		> 400 (at average cruise speed of 100 km/hr)
Engine type		Subaru 2.2L
Tank capacity (litres)		120 (+ 5 litres reserve)
Speed (km/hr)		50 to 150 (ave. 100 on line)
Landing distance		5 to 30 m
Speed (VNE) (km/hr)		160
Size	Length	4 m
	Width	1.6 m
	Height	2.6 m
Weight	MTOW	680 kg
	Empty	400 kg
	Useful	280 kg

Table 2. Salient technical specifications of GyroLAG fixed-wing aviation platform.

Number of seats		4
Endurance (hrs)		5.5
Fuel consumption (litres/hr)		42
Aircraft range (km)		>500
Engine type		Piston normally aspired - Lycoming
Tank capacity (litres)		238
Speed (km/hr)		90-220
Landing distance		250
Speed (VNE) (km/hr)		320
Size	Length	7.2 m
	Width	9.4 m
	Height	1.9 m
Weight	MTOW	1043 kg
	Empty	635 kg
	Useful	408 kg

Sensors

For reflectometry measurement, we used a classical geodetic receiver LEICA GR25 multi-frequencies and multi-constellation (for GPS: L1 C/A, L2P, L2C, L5 wavelengths; for GLONASS: L1 C/A, L2P, L2C; for GALILEO: E1, E5a, E5b, AltBOC; BeiDou B1, B2, B3, QZSS: L1, L2c, L5). This receiver is also compatible with SBAS (WAAS, EGNOS, GAGAN, MSAS) information. The maximum sampling rate was set up to 20 Hz. A standard data streaming: RTCM, NMEA, RINEX was selected. The electrical consumption is only 3.1W. This receiver was associated to a LEICA AR10 antenna that can acquire all the classical GNSS signals (Table 3).

Table 3: Existing and proposed GNSS signal detectable by the LEICA AR10 antenna (From Darrozes *et al.* 2016).

<i>System</i>	<i>L1/E1/E2/B1</i>	<i>L2/B2</i>	<i>L5/E5</i>	<i>E6/B3</i>
GPS	1575.42	1227.6	1176.45	
GLONASS	1598.063 - 1605.375	1242.938 - 1248.625		
Galileo	1575.42		1176.45, 1207.14, 1191.795	1278.75
Compass	1561.098, 1575.42, 1589.742	1207.14	1176.45	1268.52
QZSS	1575.42	1227.6	1176.45	1278.75
SBAS	1575.42			
OmniSTAR and CDGPS	1525 - 1560			

To retrieve an accurate volumetric moisture level, it is critical to acquire the complete antenna gain pattern for both Right Hand Circular Polarization (RHCP) and for the Left Hand Circular Polarization (LHCP). Fig. 1b shows the complete antenna gain for both polarization for L1. One can observe the LHCP component is higher than the RHCP component in the lower hemisphere of the antenna gain pattern which permit to obtain accurate results in reflectometry.

Airborne results and discussion

Airborne trial conditions

The two antennas and receiver have been installed on-board a fixed-wing aircraft and a gyroplane. One antenna (RHCP) was located on the top of the cockpit (fixed-wing aircraft) and top of the nose (gyroplane) to receive the direct GNSS signal. Another antenna (LHCP) was installed below the aircraft to receive the reflected GNSS signal.

The flights were performed at 120 and 140 km/hr and at 50 and 100 m agl for the fixed-wing aircraft and gyroplane respectively, following a random pattern (see yellow path in Fig. 5) over agricultural lands with two types of soil (clayed vs. sandy), various maize fields (with crop at different growth stages), a water body and flooded areas near Potchefstroom dam.

Initial airborne results

Both direct and reflected signal have been recorded and the GNSS-R data processing chain, initially set for static measurement on the ground, has then been adapted for the dynamic context of the airborne application. The preliminary results enable to distinguish high and low reflectivity areas (see Fig. 5, specular points) which have been compared with satellite imagery as well as some punctual *in situ* measurements of soil moisture in order to validate the results.

Spatial resolution of 45 m (see Fig. 5) was achieved for the specific test conditions (120-140 km/hr flying speed and 50-100 m agl survey height).

The soil moisture *in situ* measurements poorly correlated (less than 75%) to the airborne measurements. This poor correlation is due to the location of the soil sample away from the main flight path. The soil moisture indicated in Fig. 5 was then established using the measurement over the lake (used as proxy for 100% of volumetric moisture) and the road (used as proxy for 0% of volumetric moisture) and assuming the relationship is linear. In Fig. 5 inset, moisture at around 10-20 % represents 'dry' ground, and 20-30% 'wet' ground. Moisture content at 20-30% is related to vegetal cover.

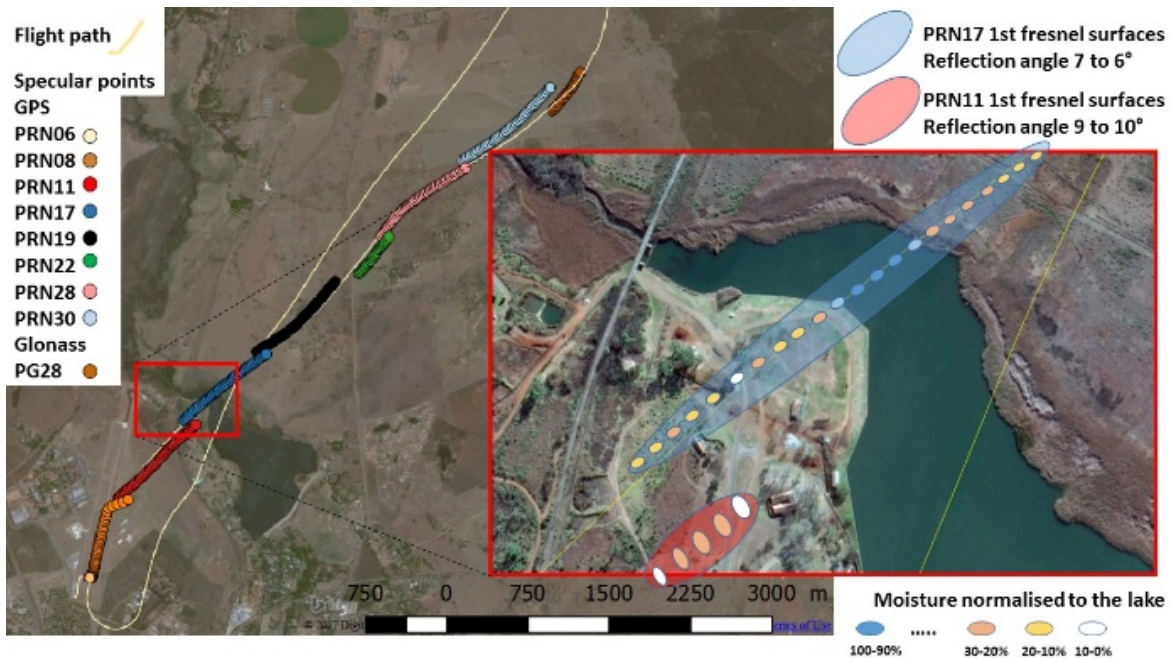


Fig. 5 Specular points over the survey flight path (yellow line) superimposed over Google Earth image. Inset: zoom into GPS PRN17 (blue) and PRN11 (red) areas with estimates of moisture content normalized to lake

Conclusions

The trial demonstrated the practical character of low level flying airborne soil moisture measurement and monitoring using GNSS reflectometry on board light and affordable fixed-wing and rotary aircraft types. The data processing chain for the dynamic conditions of airborne platform was adapted successfully from algorithm established for ground/static conditions. A second test will now be planned focusing of ground truthing with extended soil moisture *in situ* measurements.

Acknowledgments

This project is a collaboration between GyroLAG (Pty) Ltd (South Africa) and GET (France) and form part of GyroLAG's 'X-Farm' research and development program in airborne geophysics for precision agriculture applications (see Ameglio and Jacobs 2015).

References

Ameglio, L. & Jacobs, G. (2015). 'X-farm' research program: advent of airborne agro-geophysics. 14th SAGA Biennial Technical Meeting and Exhibition.

Chew ,C., Small, E., Larson, K., & Zavorotny, V. (2014). Effects of near-surface soil moisture on GPS SNR data:

***Proceedings of the 14th International Conference on Precision Agriculture
June 24 – June 27, 2018, Montreal, Quebec, Canada***

- Development of a retrieval algorithm for soil moisture. IEEE TGRS, vol. 52, no. 1, pp. 537-543.
- Darrozes J., Roussel N. & Zribi M. (2016). The Reflected Global Navigation Satellite System (GNSS-R): from theory to practice. Chapter 7, vol 2, 1st Edition Ed. Baghdadi, Zribi.
- Darrozes, J., Dufrechou, G., Minh Ha, C., Varias, N., Pibouleau, R., Soriano, M., Ramillien, G. & Frappard, F. (2017). Can GNSS-R be used to monitoring and mapping mining waste deposit and its associated contamination? Unpublished internal report, 6 p.
- Dorigo, W.A., Xaver, A. Vreugdenhil, M. Gruber, A., Hegyiová, A. Sanchis-Dufau, A.D., Zamojski, D., Cordes, C., Wagner, W. & Drusch, M. (2013). Global Automated Quality Control of In situ Soil Moisture data from the International Soil Moisture Network. Vadose Zone Journal, doi: 10.2136/vzj2012.0097.
- Kerr, Y., Waldteufel, P., Wigneron, J.P., Delwart, S., Cabot, F., Boutin, J., Esocrihuela, M.J., Font, J., Reul, N., Gruhier, C., Juglea, S., Drinkwater, M., Hahne, A., Martin-Neira, M. & Mecklenburg, S. (2010). The SMOS mission: New tool for monitoring key elements of the global water cycle. IEEE, vol. 98, no. 5.
- Larson, K.M, Small, E.E., Gutmann, E., Billich, A., Axelrad, P. & Braunn, J. (2007). Using gps multipath to measure soil moisture fluctuations: initial results. GPS Solution, vol. 12, pp. 173-177.
- Morisette J. T., Baret F., Privette J. L. *et al.* (2006). Validation of global moderate-resolution LAI products: A framework proposed within the CEOS land product validation subgroup. IEEE Transaction on Geoscience and Remote Sensing, 44, 7, 1-13.
- Motte, E., Zribi, M., Fanise, P., Darrozes, J., Egido, A., Baghdadi, N., Baup, F., Frison, P.-L., Guyon, D., Wigneron, J.-P. (2016a). GLORI: A GNSS-R dual polarization Airborne Instrument for Soil Moisture and Vegetation Monitoring. SENSING.
- Motte, E., Roussel, N., Boniface, K. & Frappard, F. (2016b). Applications of GNSS-R in Continental Hydrology. In Land Surface Remote Sensing in Continental Hydrology, Chapter 9, 1st Edition, Ed. Baghdadi, Zribi.
- Roussel, N., Frappard, F., Ramillien, G., Darrozes, J., Baup, F., Lestarquit, L. & Ha, C.M. (2016). Detection of soil moisture variations using GPS and GLONASS SNR data for elevation angles ranging from 2° to 70°. IEEE JSTARS, 4781 – 4794. Doi: 10.1109/JSTARS.2016.2537847.
- Roussel, N. (2015). Application de la réflectométrie GNSS à l'étude des redistributions des masses d'eau à la surface de la Terre, Instrumentation et méthodes pour l'astrophysique. astro-ph.IM. Toulouse, Université Paul Sabatier - Toulouse III. Doctoral thesis, 285 p.